International Journal of Mass Spectrometry 277 (2008) 262–268

Contents lists available at ScienceDirect

International Journal of Mass Spectrometry

journal homepage: www.elsevier.com/locate/ijms

Chemistry induced by low-energy electrons in condensed multilayers of pure small organic acids

I. Martin[a], M. Bertin[b,c], A. Domaracka[d], R. Azria[b,c], E. Illenberger[a], A. Lafosse[b,c,*]

[a] Institut für Chemie und Biochemie - Physikalische und Theoretische Chemie, Freie Universität Berlin, Takustrasse 3, D-14195 Berlin, Germany
[b] Laboratoire des Collisions Atomiques et Moléculaires (FR LUMAT),
University Paris-Sud, UMR 8625, Orsay F-91405, France
[c] CNRS, Orsay, F-91405 Orsay, France
[d] Atomic Physics Group, Faculty of Applied Physics and Mathematics, Gdansk University of Technology, ul. Narutowicza 11/12, 80-952 Gdansk, Poland

ARTICLE INFO

Article history:
Received 11 April 2008
Received in revised form 3 June 2008
Accepted 4 June 2008
Available online 11 June 2008

Keywords:
Electron induced interaction
Synthesis reaction
High resolution electron energy loss spectroscopy (HREELS)
Dissociative electron attachment
Selective decarboxylation

ABSTRACT

Electron-induced decarboxylation in condensed films of formic acid HCOOH, partially deuterated acetic acid CH_3COOD and trifluoroacetic acid CF_3COOH, has been studied in the energy range 0.7–20 eV by high resolution electron energy loss spectroscopy (HREELS). The yield of carbon dioxide formation shows a peak around 1 eV irradiation energy associated with a resonant mechanism involving the transient negative ion $[RCOOH]^{\#-}$ and an essentially non-resonant contribution increasing with irradiation energy above an onset located in the range 6–9 eV, depending on the carboxylic acid under consideration. The remarkable point of this study is that it is possible to selectively control the decarboxylation reaction by tuning the electron energy of irradiation.

1. Introduction

Low-energy electrons ($E_i < 30$ eV) play a major role in many different applications and techniques such as plasma chemistry [1–3], radiation chemistry and biology [4–8], particle beam [9,10] and photon [11,12] induced surface chemistry. Upon interaction with condensed molecules, electrons drive bond cleavage thus generating a population of very reactive species in the condensed medium. These species may interact either within the film to synthesize new molecules or form a chemical bond with the substrate surface. The former reaction is known as electron-induced synthesis and the latter as electron-induced surface functionalization. Bond cleavage may involve neutral or ionic dissociation mechanisms and at lower energy ($0 < E_i < 20$ eV) dissociative electron attachment (DEA). DEA implies the formation of a transient negative ion that can be viewed as a molecular quantum state embedded in the electron-target continuum [13–16]. In a molecular film the extra electron will be generally localized on an individual molecule, the interaction can therefore be regarded as taking place on a molecular site. Low-energy electrons are then capable of chemical selectivity [17–20] in contrast to high energy ones, due to the large number of open dissociative channels in the latter case and their non-resonant nature.

Accordingly, low-energy electrons have attracted considerable interest in the past few years due to their potential to induce specific chemical reactions in pure ices condensed at cryogenic temperature. For instance, it has been shown that electron irradiation leads to the formation of ozone (O_3) in condensed oxygen (O_2) [21], of chlorine (Cl_2) in chlorofluoroalkanes [22–24], and of carbon monoxide (CO) in condensed acetone (CH_3COCH_3) [25], methanol (CH_3OH) [26], and carbon dioxide (CO_2) [27]. In the case of ozone and chlorine formation, a resonant process involving electrons of subexcitation energies was established, whereas the formation of carbon monoxide was observed to take place above a threshold of 8 eV with a maximum around 16 eV. This CO production was discussed in terms of (i) formation of several core-excited resonances, which may lead directly to the fragmentation of the molecule via DEA, (ii) neutral dissociation resulting from the excitation (via direct excitation or via resonant scattering) into an entirely repulsive part of a neutral-excited state, and (iii) non-resonant dissociative ionization. Recently, electron-induced decarboxylation of small organic acids RCOOH (R=H, CH_3 and CF_3), was observed to occur in the condensed phase by temperature programmed desorption (TPD) analysis with increasing efficiency above 8–9 eV in

---

[*] Corresponding author. Tel.: +33 1 69 15 76 98.
E-mail address: anne.lafosse@u-psud.fr (A. Lafosse).

1387-3806/$ – see front matter © 2008 Elsevier B.V. All rights reserved.
doi:10.1016/j.ijms.2008.06.003

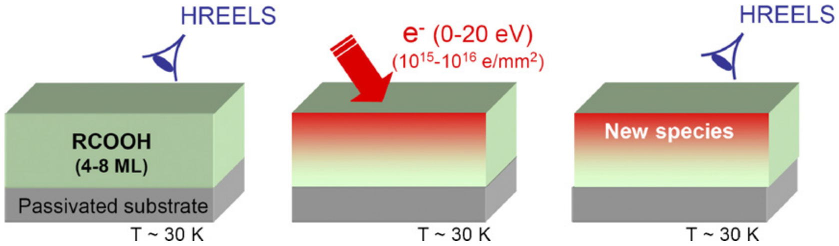

Fig. 1. Principle of the experimental procedures for studying electron-induced chemistry within the condensed film. A molecular film is prepared by vapour deposition on the passivated substrate cooled down to ~30 K. It is then irradiated using low-energy electrons of tuneable energy (0–20 eV) and dose (10^{15}–10^{16} e^-/mm^2). The result of the electron writing procedure is probed by HREEL vibrational spectroscopy directly at ~30 K.

the group of Illenberger [28,29][1], indicating that the involved reactions are initiated via electronically excited neutral states rather than negative ion resonances.

The study of electron-induced reactivity in condensed organic acids RCOOH is important in the contexts of fundamental studies and the development of applications. First the —COOH organic group is present in a number of biological molecules such as amino and fatty acids, small organic acids are found in the interstellar medium [30,31] and their radiation-induced chemistry participates in the formation of organic molecules. Second, to elaborate functionalized semi-conductor substrates suitable for sensor development, chemisorbed —COOH groups are typically used as anchors for further selective immobilization of complex molecules on a substrate [32,33]. Thus, the understanding of the chemistry induced by primary or secondary low-energy electrons on molecular objects, which contain an acidic function, is a necessary step to control radiation-induced damage, as well as electron-induced functionalization.

In this paper, we report on electron-induced decarboxylation in three acids, formic acid HCOOH, partially deuterated acetic acid CH_3COOD and trifluoroacetic acid CF_3COOH, in the energy range 0.7–20 eV using high resolution electron energy loss spectroscopy (HREELS). In this technique, electrons with a given energy (usually in the range below 10 eV) impinge on a target and the backscattered electrons are collected as a function of their energy. The obtained spectra show peaks which are the fingerprints of the vibrational modes of localized functional groups belonging to a particular molecule. This technique is known to be very surface sensitive [34]. We will demonstrate that the yield of carbon dioxide formation shows a peak around 1 eV irradiation energy associated with a resonant state $[RCOOH]^{\#-}$ and a non-resonant contribution with an onset, located in the range 6–9 eV depending on the carboxylic acid under consideration. In addition, the formate anions $HCOO^-$ were clearly observed after electron irradiation at 1 eV of condensed formic acid. The influence of the degrees of aggregation on the reactivity of slow electrons with molecules was demonstrated and extensively studied in the group of Illenberger in Berlin [35,36]. Thus special attention is given to trifluoroacetic acid, following the experiments performed on electron driven reactions in single gas phase molecules [37], in molecular clusters generated by supersonic beam expansion [38], and in the condensed phase by electron stimulated desorption (ESD) of anions and TPD [29]. The present HREELS study demonstrated that electron irradiation at 1 and 20 eV leads to the complete destruction of the CF_3COOH molecules, while irradiation at 2.5 and 7 eV leaves the films unchanged. Indications for the formation of water molecules H_2O driven by electron irradiation were obtained, whereas no clear indications for small fluorinated fragments and products were observed.

2. Experimental apparatus

The principle of the experimental procedure is given in Fig. 1. The experiments were performed in a ultra-high vacuum chamber (base pressure below 5×10^{-11} Torr) equipped with a liquid helium flow cryostat, an electron gun and a HREEL spectrometer. The substrate of hydrogenated polycrystalline diamond [39], on which the ice films were deposited, is chemically inert, thus preventing contribution(s) of direct reaction(s) between the condensed species and the substrate surface, as checked by verifying that the vibrational signature of the substrate was not changed after condensation and subsequent evaporation of the film. The sample is fixed to the cold end of a cryostat and cooled down to 30 ± 5 K. Molecular films are prepared by exposing the cooled substrate to a partial pressure of 1×10^{-8} Torr typically during 800 s (for a 8 L dose), resulting in deposition of about 8 monolayers (ML). The samples are irradiated using an electron gun, which supplies, depending on the electron energy, a current of 2–40 μA on an average area estimated to ~2 mm^2, with a resolution of about 300 meV. Exposures of typically 10^{15}–10^{16} e^-/mm^2 (uncertainty estimated to 50%) were used for ice processing, corresponding to electron fluxes roughly estimated to 0.5–15 e^-/s per molecule and total doses of about 100–1000 electrons per molecule. Chemical modifications are probed directly at 30 ± 5 K. The sample surface is explored by changing its position in the HREEL collision chamber in order to ascertain the localization of the irradiation spot and to probe the induced chemical changes over its whole area. The HREEL spectrometer consists of a double monochromator and a single analyzer (model IB 500 by Omicron). The presented energy loss spectra were obtained at an incident electron energy of 5 eV in the specular geometry, with an incident direction of 55° with respect to the surface normal and an overall resolution of 6 meV, measured as the full width at half maximum of the elastic peak.

Identification of the products synthesized under electron irradiation is performed by comparing the newly observed energy losses directly with the HREEL spectra of condensed products, namely carbon dioxide CO_2 and water H_2O in the case of irradiated organic acids. Mechanisms of induced reactions are deduced from the qualitative evolution of the product formation efficiency as a function of irradiation energy and from the dissociations previously identified in gas and condensed phases, since the primary step of the reaction has to be initiated either by electron attachment leading to the formation of a transient negative ion (TNI) or by non-resonant electron-induced bond breaking.

Formic acid HCOOH was purchased from Riedel-deHaën (99.9%), partially deuterated acetic acid CH_3COOD from Sigma–Aldrich (99%) and trifluoroacetic acid CF_3COOH from Fluka (purity > 99.5%). To compare the spectra of the irradiated acid films with that of possible reaction products, water H_2O of high purity (Normapur, >99.9%) and pure carbon dioxide CO_2 (CAL-gas, 100%) were used. All the acids and water were purified by freeze-pump-thaw cycles and degassed under vacuum before dosing onto the cold substrate.

---

[1] R. Balog, E. Illenberger, private communication.

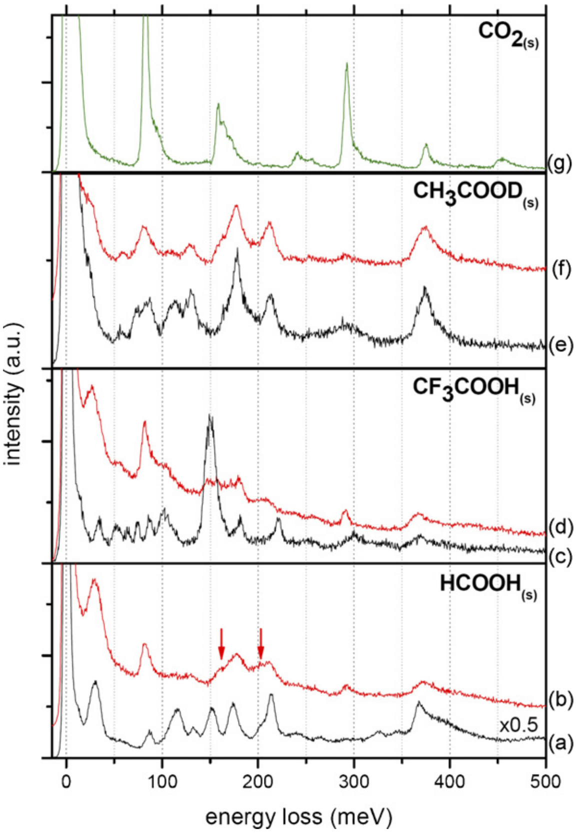

Fig. 2. Energy loss spectra of RCOOH films after electron irradiation at low energy 0.7 and 1 eV compared to the freshly deposited films: multilayer film (8 ML) of formic acid HCOOH before (a) and after irradiation (b) (1 eV, 3.4×10^{15} e^-/mm^2); multilayer film (4 ML) of trifluoroacetic acid CF_3COOH before (c) and after irradiation (d) (1 eV, 13×10^{15} e^-/mm^2); multilayer film (8 ML) of partially deuterated acetic acid CH_3COOD before (e) and after irradiation (f) (0.7 eV, 3.6×10^{15} e^-/mm^2). In the panel dedicated to formic acid, the arrows indicate the features located at 161 and 202 meV ascribed to the anion $HCOO^-$. The energy loss spectrum of a multilayer film (8 ML) of carbon dioxide CO_2 (spectrum (g)) is given for comparison.

Nevertheless, the co-deposition of CH_3COOH with the partially deuterated associated species CH_3COOD could not be excluded because of possible isotope exchange on the gas inlet walls.

3. Results and discussion

Energy loss spectra of pure films of freshly deposited carboxylic acids HCOOH, CH_3COOD and CF_3COOH are shown in Fig. 2 (spectra (a), (c) and (e), respectively). The resolution achieved in HREEL spectroscopy does not allow us to resolve all the contributions, so that the observed losses often result from the overlapping of several vibrational modes. Furthermore for multilayer films, HREEL spectra consist of losses attributed to fundamental vibrational modes, broad features at low-energy loss (∼20–35 meV) ascribed to overlapping lattice modes of the film molecular network, and multiple losses originating from electron multiple scattering and/or combination and harmonic modes. Attributions of the observed losses are done according to published HREEL vibrational spectra [40–43] and infra-red (IR) spectroscopy data [30,44–49]. Assignments of the observed energy loss peaks are summarized in Tables 1–3 for formic acid HCOOH, partially deuterated acetic acid CH_3COOD and trifluoroacetic acid CF_3COOH, together with a selection of relevant data reported in the literature. The carboxylic acid films cannot be viewed as an assembly of single molecules coupled by weak intermolecular forces. From the tendency of the present acids to form O···H—O, O—D···O bridges, we can rather expect that the films and their surfaces consist of molecular networks coupled by comparatively stronger hydrogen bonds [29,41]. When oxygen atoms from the C=O bonds are involved in hydrogen bonding with the hydrogen atoms of the acid groups (—COOH), the energy loss feature attributed to the stretching modes of the OH (OD) bonds is broadened and strongly shifted towards low-energy losses.

The energy loss spectrum recorded for a freshly deposited multilayer film of formic acid HCOOH is dominated by losses attributed to the vibrational modes of the C—H bond and to the acidic function COOH, respectively and is in very good agreement with the IR spectrum measured by Bisschop et al. [30]. The stretching ν(CH), bending δ(CH) and out-of-plane π(CH) modes are observed at 368, 174, and 132 meV. The stretching modes ν(C=O) and ν(C—O) of the acid groups give rise to the peaks located at 214 and 151 meV, respectively and the bending mode δ(O—C=O) to a peak at 87 meV. Stretching modes ν(OH) of OH groups involved in hydrogen bonds give rise to a structured band, containing two resolved peaks at 325 and 346 meV, and to a shoulder at ∼390 meV, unresolved from the loss attributed to the mode ν(CH). Multiple scattering contributes also to the two former losses ($2 \times \delta$(CH) and δ(CH) + ν(C—O)). The out-of-plane bending mode π(OH) is observed at 116 meV.

Partially deuterated acetic acid CH_3COOD, rather than CH_3COOH, was chosen, because losses related to stretching modes of OH bonds involved in a hydrogen bridge network are overlapping with the broad band centred at 374 meV, attributed to the stretching modes of methyl group $\nu_a(CH_3)$ and $\nu_s(CH_3)$. The asymmetric bending mode $\delta_a(CH_3)$ is observed at 177 meV, and the symmetric one $\delta_s(CH_3)$ together with the stretching mode ν(C—O) are assigned to the unresolved shoulder at ∼165 meV. The losses located at 130 and 113 meV are attributed to the rocking modes of the methyl group $\rho(CH_3)$ and the stretching mode ν(CC), respectively. The most characteristic loss related to the acidic function —COOD is resolved at 214 meV and is attributed to the stretching mode of the carbonyl group ν(C=O). The broad band centred at 295 meV is ascribed to stretching modes of OD groups involved in hydrogen bridges. Assignments of the vibrational modes to localized functional groups vary in the literature, in particular, due to intermixing of group modes below 100 meV [41,43,46]. The bending modes γ(OD) and δ(OCO) contribute to the losses located at 85 and 73 meV, and the loss at 56 meV is attributed to the rocking mode ρ(OCO). Co-deposition of CH_3COOH when preparing a film of partially deuterated acetic acid cannot be excluded, since isotopic exchange on the gas inlet walls cannot be avoided. However, losses related to the fully hydrogenated species cannot be isolated: losses attributed to stretching modes ν(OH) are overlapping with the feature attributed to $\nu(CH_3)$ and could account for the shoulder seen on the high-energy loss side of the related feature, the bending modes δ(COH) and γ(OH) are expected to contribute to the HREEL spectrum at similar energy losses than $\delta_a(CH_3)$ and ν(CC), respectively.

The energy loss spectrum recorded for a freshly deposited CF_3COOH film is strongly dominated by a peak located at about 150 meV, as already observed by Parker et al. at an incident electron energy of 1.3 eV for multilayers of CF_3COOH condensed at 90 K [42]. The acidic group related features are observed as a broad band centred at 369 meV and attributed to the stretching mode ν(OH) of the hydrogen bonded OH groups. Three resolved losses at 219, 180 and 86 meV are attributed, respectively, to the stretching modes ν(C=O) and ν(C—O) of double and single CO bonds, and the bending mode δ(OCO) (although an overlapping contribution of the $\delta(CF_3)$ mode cannot be excluded, see Table 3). The dominant broad peak at 150 meV results from the overlapping contributions of the stretching modes of the trifluoromethyl group and will be referred to as $\nu(CF_3)$ in the following. The peaks at

Table 1
Energies (meV) and mode assignments of losses observed in the HREEL spectrum of HCOOH multilayers (8 ML) condensed at 30 ± 5 K

Mode	IR, α-crystal HCOOH(s), $T \sim 77$ K [44]	IR, Monomer HCOOH(g) [44,49]	HREELS, HCOOH(cond), $T \sim 110$ K [40]	FTIR, HCOOH(cond), $T \sim 15$ K [30]	HREELS, HCOOH(cond), $T \sim 30 \pm 5$ K (this work)
ν(CH)	367	365	367	366	368
ν(OH)	314	443	324	386	390 (*) (m)
				341	346 (m)
				320	325
ν(C=O)	211	219	212	213	214
	199		204	205	205 (*)
δ(CH)	172	172	173	172	174
	171				
	170				
δ(OH)	193	152			
ν(C—O)	156	137	151	150	151
	152				
π (CH)	134	128		133	132
π(OH)/τ	121	79	119	115	116
δ(OCO)	89	77–79	88	87	87
Lattice modes					30

Published IR and HREELS data on vibrational modes observed for HCOOH as monomer, dimer/catemer/chain are given for comparison. Keys: ν: stretching, δ: bending, π: out-of-plane bending. (*) Unresolved. (m) Loss resulting from several contributions. The following contributions are, nevertheless, expected as minor ones. ~346 meV: also 2δ(CH); ~325 meV: also ν(C—O) + δ(CH); ~395 meV: ν(CH) + lattice; ~265 meV: also π(OH) + ν(C—O); ~244 meV: ν(C=O) + lattice.

lower energy loss can be attributed to deformation modes of the CF_3 group and skeleton modes. Additional peaks of lower intensity are ascribed to multiple scattering involving $\nu(CF_3)$ modes (see Table 3).

Energy loss spectra recorded after electron irradiation at 1 eV for multilayer films of formic acid HCOOH (spectrum (b)), trifluoroacetic acid CF_3COOH (spectrum (d)) and after electron irradiation at 0.7 eV of a multilayer film of partially deuterated acetic acid CH_3COOD (spectrum (f)) are compared with the spectra recorded for the freshly deposited films in Fig. 2. All these spectra display significant changes. In particular, (i) ν(C=O) related losses are reduced in intensity in irradiated films (especially for HCOOH and CF_3COOH; the intensity decrease is not so obvious in the case of CH_3COOD, which is not understood), whereas two new losses at 82 and 292 meV and an unresolved shoulder at about 158 meV appear, (ii) in the formic acid HREEL spectrum the CH related losses and the peak attributed to the out-of-plane bending π(OH) almost disappears, (iii) in CH_3COOD irradiated film the intensities of the ν(CC) and γ(OD)/δ(OCO) related peaks decrease, (iv) and in the trifluoroacetic acid irradiated spectrum all the skeleton and CF_3 related losses in the range 20–170 meV have vanished. The new peaks at 82 and 292 meV are associated to CO_2 formation as demonstrated by comparing the new observed losses with the spectrum recorded for a film of pure carbon dioxide, reported in the upper panel of Fig. 2 (spectrum (g)) for comparison and discussed in detail elsewhere [50]. The losses are attributed to the fundamental bending δ (82 meV) and asymmetric stretching ν_{as} modes of CO_2 (292 meV), and the unresolved shoulder to the Fermi resonance combining the symmetric stretching with the overtone 2δ of the bending mode (158 meV) [51,52].

Table 2
Energies (meV) and mode assignments of losses observed in the HREEL spectrum of CH_3COOD multilayers (8 ML) condensed at 30 ± 5 K

Mode	RAIRS, CH_3COOH(cond), $T \sim 100$ K [45]	RAIRS, CH_3COOH(cond), $T \sim 100$ K [46]	IR, solid CH_3COOH(s) [46]	HREELS, CH_3COOH(D)(cond), $T \sim 170$ K [41]	HREELS, CH_3COOD(cond), $T \sim 30 \pm 5$ K (this work)
$\nu_a(CH_3)$		371		368	374
$\nu_s(CH_3)$		363			365 (*)
ν(OH)		375	364	313	
ν(OD)		285 $^{(D)}$	274 $^{(D)}$	247	295
		277 $^{(D)}$	272 $^{(D)}$		
ν(C=O)	222	222	213	209	214
	215	215	206		
δ(COH)	178	178	174		
$\delta_a(CH_3)$	176	176		177	177
$\delta_s(CH_3)$	169	169	169		165 (*)
ν(C—O)	163	163	157	162	
$\rho_a(CH_3)$	130	131	130		130
$\rho_s(CH_3)$	127	127	126		
ν(C—C)	111		110	118	113
γ(OH)	119	119	112		
γ(OD)			83 $^{(D)}$	87	73
δ(OCO)			78	85	
ρ(OCO)			59		56
δ(CCO)			56		
Lattice modes				31	~23 (*)

IR and HREELS data on vibrational modes observed for CH_3COOH(D) condensed molecular film and as solid are given for comparison. Keys: a: asymmetric, s: symmetric, ν: stretching, δ: bending, ρ: rocking, γ: out-of-plane bending. (*) Unresolved. $^{(D)}$ Vibrational mode of CD_3COOD reported in the same reference.

Table 3
Energies (meV) and mode assignments of losses observed in the HREEL spectrum of CF_3COOH multilayers (4 ML) condensed at 30 ± 5 K

Mode	IR, CF_3COOH in Ne matrix [47]	IR, cyclic $(CF_3COOH)_2$ in Ne matrix [47]	IR, catemer $CF_3COOH(s)$ [48]	HREELS, CF_3COOH(cond), $T \sim 90$ K [42]	HREELS, CF_3COOH(cond), $T \sim 30 \pm 5$ K (this work)
ν(OH)	444	362	362	374	369 (m)
ν(C=O)	226	221	219	221	219
ν(C—O)	176	183	183	186 (a)	180
δ(COH)	139	163	163, 162	150 (a)	161 (*)
$\nu(FCF_2)$	155	154	152	150	153 (*)
ν(FCF)	150	148	148		149
$\nu(CF_3)$	147	146	147, 145		
τ(OH)	72	115	112, 110		~108 ? (*)
ν(CC)		103	103	110	100
$\delta(CF_3)$	82	85	96		100, 86 (b)
δ(OCO)	97	88	89	88	86
$\delta(FCF_2)$	73	75 (b)	76		73
δ(FCF)	62	64 (b)	64		63
$\omega_{antigear}$		57	57		52
$\rho_{antigear}$		48	50	50	
ω_{gear}	30, 31	30	37		33
ρ_{gear}		30	32	37	

IR and HREELS data on vibrational modes observed for CF_3COOH as monomer, dimer and catemer are given for comparison. Mode assignments in terms of group vibrational frequencies have been taken from [48]. Keys: ν: stretching, δ: bending, ρ: rocking, τ: torsion, ω: wagging, see Ref. [48] for details. (*) Unresolved. (a) The attribution proposed by Parker et al. has been changed to be in accordance with the assignment proposed by Berney. (b) Contribution to the loss at 100 or 86 meV possible, depending on the presence of monomers, dimers or catemers. (m) Contributions of multiple scattering: $2\nu(CF_3)$ and $3\nu(CF_3)$ at ~300 and 450 meV, $\nu(CF_3) + \nu(C{=}O)$ at ~369 meV, $\nu(CF_3) + \nu(C{-}O)$ at ~330 meV, $\nu(CF_3) + \nu(CC)/\delta(CF_3)$ at ~250 meV, $\nu(CF_3) + (\omega/\rho)_{antigear}$ at ~202 meV.

Electron irradiation for these three acids was performed at increasing irradiation energy up to 20 eV to gain insights into the mechanisms leading to decarboxylation. Generally, a set of data corresponding to five to six irradiation energies was measured for each compound, the values being chosen taking into account published data on DEA in the gas phase, so that the irradiation energy values characterizing the different reaction regimes are evaluated with an uncertainty estimated to ±1 eV. The general qualitative efficiency for CO_2 formation schematized in Fig. 3 as a function of the irradiation energy could be deduced. For the three acids, it consists of a peak located around 1 eV and an increasing contribution at higher irradiation energy with an onset located in the range 6–9 eV, depending on the carboxylic acid under consideration. Thus two different regimes can be distinguished: a resonant one around 1 eV and an essentially non-resonant one above 6–9 eV. The latter high-energy regime was already observed by TPD mass analysis [28–29][1] but the low-energy regime could only be shown when using HREEL spectroscopy, a method known to be quite sensitive.

At low energy the only known electron-induced process in carboxylic acids RCOOH is resonant electron attachment leading to the formation of a TNI $[RCOOH]^{\#-}$, as deduced from gas phase experiments [53–55]. In our experimental conditions, the electron flux is low enough to exclude the contribution of an interaction between the transient negative ion $[RCOOH]^{\#-}$ and a further incoming electron. The resonant state decays either by electron autodetachment or by DEA reactions. The main DEA products are the anion $(M{-}H)^-$ (where M is the RCOOH molecule, [53,56,57]), together with $(CH_2CO_2)^-$ [58] in the case of acetic acid, and $(CF_2CO_2)^-$ and CF_2^- in the case of trifluoroacetic acid [37]. The hydrogen abstraction decay channel is shown in the energy loss spectrum of the irradiated formic acid by the contributions located at 161 and 202 meV, which can be attributed to CO_2^- related vibrational modes of the formate anion $HCOO^-$ [49,59].

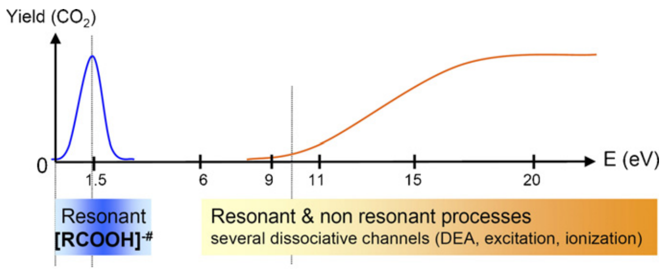

Fig. 3. Qualitative efficiency for CO_2 formation in pure carboxylic acid RCOOH films is represented schematically as a function of the electron irradiation energy. The relative intensities of the resonant feature located around 1 eV and of the asymptotic level achieved by the increasing contribution of the resonant and non-resonant competitive processes have been artificially set as equal and should not be compared. The onset value for a noticeable contribution of the high-energy processes is located in the range 6–9 eV, depending on the nature of the R group of the organic acid RCOOH.

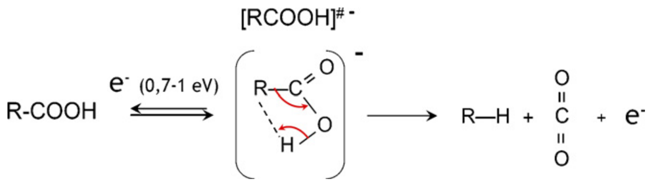

Fig. 4. Concerted mechanism proposed for the decarboxylation of small organic acids RCOOH induced by electron irradiation at 0.7–1 eV: the incoming electron is first attached to the molecule and the transient negative anion undergoes then internal rearrangements presumably resulting in a hydrogen addition to the R group accompanied by the formation of carbon dioxide.

Moreover, for all the considered acids the reaction $R{-}COOH + e^- \rightarrow CO_2 + R + H + e^-$ is endothermic, as well as the reaction leading to the formation of the anion CF_3^- by attachment of the extra electron in the particular case of trifluoroacetic acid. Accordingly, a concerted mechanism is proposed and schematized in Fig. 4. This mechanism assumes that the most probable co-products are molecular hydrogen H_2, partially deuterated methane CH_3D and trifluoromethane CF_3H, respectively, and the reaction enthalpies can then be evaluated for the gas phase [28,29,37,49,58].[2]

$$HCOOH + e^- \rightarrow CO_2 + H_2 + e^- \quad \Delta_r H(g) \sim -0.15\,\text{eV}$$

---

[2] depending on the value taken for $\Delta_f H^\circ(CF_3COOH)$ [49].

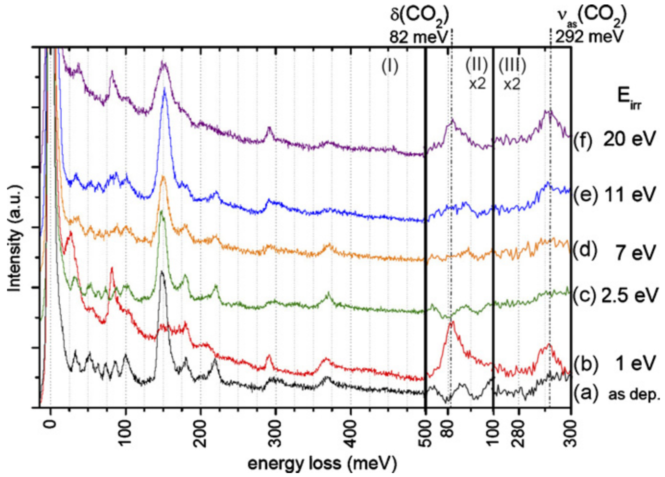

Fig. 5. Electron energy loss spectra of multilayer (4 ML) films of trifluroacetic acid CF_3COOH before (a), and after electron irradiation at increasing energies E_{irr} = 1 eV (b), 2.5 eV (c), 7 eV (d), 11 eV (e) and 20 eV (f). Complete spectra are presented in the panel (I), and the two regions 70–100 meV and 270–300 meV, in which losses attributed to the bending mode $\delta(CO_2)$ and to the asymmetric stretching mode $\nu_{as}(CO_2)$ are expected, are magnified in panels (II) and (III), respectively. In the latter two panels intensities were multiplied by a factor 2 and vertical shifts were adapted for clarity reasons.

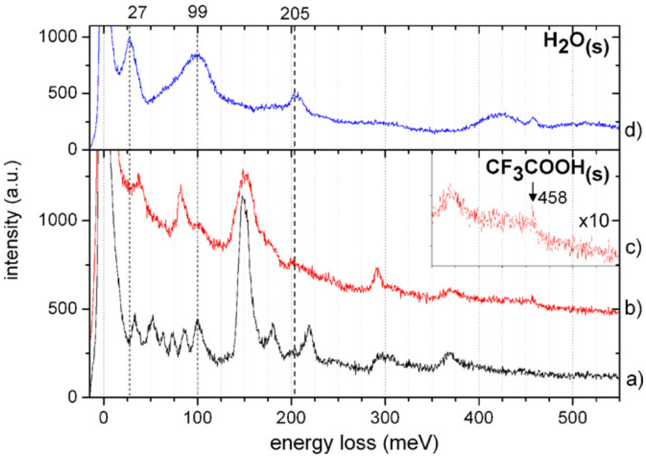

Fig. 6. Energy loss spectra of a film (4 ML) of pure trifluoroacetic acid CF_3COOH before (a) and after electron irradiation at 20 eV (b). The latter spectrum is magnified by a factor 10 in the energy loss range 350–550 meV in the inset (c). The energy loss spectrum of a pure film (8 ML) of water H_2O (d) is given in the upper panel for comparison.

$$CH_3COOD + e^- \rightarrow CO_2 + CH_3D + e^- \quad \Delta_r H(g) \sim -0.36\,\text{eV}$$

$$CF_3COOH + e^- \rightarrow CO_2 + CF_3H + e^- \quad \Delta_r H(g) \sim -0.61/-0.76\,\text{eV}$$

In the working conditions of temperature and pressure (30 ± 5 K, $<10^{-10}$ Torr) molecular hydrogen and methane are not trapped and desorb into vacuum upon formation, whereas CF_3H should be trapped and losses should be observed. However, no significant contribution, which could be assigned to one of the dominant CF_3 related modes of CF_3H (observed at 143 meV in the gas phase [49]) could be detected in the energy loss spectrum following irradiation at 1 eV (see Fig. 2(d) or Fig. 5(b)). This is not understood at the present time.

The remarkable point is that it is possible to selectively control the decarboxylation reaction by tuning the electron energy of irradiation. While at subexcitation energy photons are not operative agents to induce this reaction, 1 eV electrons are remarkably efficient ones. By contrast, at higher energy several primary electron-induced dissociation channels, resonant and non-resonant, can contribute to the decarboxylation reaction, excluding any selective control.

In the following, the particular case of trifluoroacetic acid CF_3COOH condensed films will be discussed since it presents additional remarkable features after electron irradiation. The influence of the degrees of aggregation on the reactivity of slow electrons with trifluoroacetic acid was investigated by comparing the results obtained on single acid molecules in the gas phase [37], on molecular clusters [38], and on condensed molecular films of CF_3COOH [29]. Electron attachment to clusters of trifluoroacetic acid revealed a variety of large complexes in addition to the ions known from DEA to single CF_3COOH molecules. In particular, the most intense signal was due to the ion–molecule complex $CF_3COO^- \cdot H_2O$ which resulted from a chemical reaction initiated by the attachment of electrons at an energy of 0.4 eV to the neutral hydrogen bonded dimer. The study in the condensed phase was conducted in Berlin by ESD analysis of the anions and by TPD [29] and in Orsay by HREELS. The energy loss spectra of trifluoroacetic acid after irradiation at various incident electron energies are shown in Fig. 5. As mentioned above, decarboxylation reaction occurs around 1 eV and above a threshold between 7 and 11 eV, whereas electron irradiation at 2.5 and 7 eV does not induce any noticeable modification of the film.

After irradiation at 1 eV, no significant contributions of intact trifluoroacetic acid molecules are observed, in particular the collection of losses in the energy loss range 20–170 meV has vanished. Most of the CF_3COOH molecules were thus destroyed upon irradiation. The vibrational modes for some possible products are tabulated for CF_2 at 152, 137–138 and 83 meV, for CF at 114 meV, for F_2 at 162 meV and for HF at 514, 488, 475 meV, depending on the degree of hydrogen bonding [49,60]. There is no evidence for these small fluorinated fragments and products.

After irradiation at 20 eV (see Fig. 6(b)) the same behaviour is observed in the region 20–120 meV and the dominant loss at 150 meV is much broader than before irradiation (its full width at half maximum increases from 14 to 22 meV) so that this loss can no longer be attributed exclusively to CF_3 related vibrational modes of CF_3COOH molecules. In addition, a remarkable small feature is observed in the irradiated film at ∼460 meV (see Fig. 6(b) and (c)), together with two smoothed shoulders at ∼99 and ∼205 meV. Accordingly, the HREEL spectrum of CF_3COOH after irradiation at 20 eV is compared to the spectrum of a multilayer (8 ML) amorphous film of pure water H_2O in Fig. 6. The two bands centred at 27 and 99 meV are attributed, respectively, to translational ν_T and librational ν_L phonon modes of the molecular network. The bending mode $\delta(H_2O)$ is assigned to the loss located at 204 meV, the broad band centred at 422 meV is ascribed to the symmetric ν_s and asymmetric ν_a stretching modes of OH bonds involved in the hydrogen bond network, and the loss at 457 meV is assigned to the stretching mode of free OH groups (located in particular at the film surface) [61,62]. Thus, there are indications for the formation of a small quantity of water molecules H_2O driven by electron irradiation.

4. Conclusion

Electron-induced decarboxylation in condensed films of three organic acids, formic acid HCOOH, partially deuterated acetic acid CH_3COOD and trifluoroacetic acid CF_3COOH, in the energy range 0.7–20 eV was studied using high resolution electron energy loss spectroscopy. The yield of carbon dioxide formation presents a peak around 1 eV irradiation energy associated with a resonant state $[RCOOH]^{\#-}$ and a non-resonant contribution increasing with the electron energy of irradiation above an onset located in the range 6–9 eV, depending on the carboxylic acid under consideration. In addition, the formation of the formate anion $HCOO^-$ was observed after electron irradiation at 1 eV of condensed formic acid and indications for the formation of water were obtained after electron irradiation at 20 eV of condensed trifluoroacetic acid.

Acknowledgments

IM, MB, AD, RA, and AL dedicate this work to Prof. Eugen Illenberger on the occasion of his 65th birthday. The authors acknowledge Dr. J. Langer, Dr. R. Balog and Dr. D. Pliszka for interesting and constructive discussions. IM and AD acknowledge support through the Marie Curie Fellowship of the European Community Program Improving Human Potential and the Socio-economic Knowledge Base under number HPMT-CT-2001-00358. The HREEL equipment was financially supported by Conseil Général de l'Essonne. This work has been partly performed within the EPIC EU Network, "Electron and Positron Induced Chemistry" (Framework V) and ESF Network EIPAM "Electron Induced Processes at the Molecular Level". Support provided by the Cost Action CM0601 "Electron Controlled Chemical Lithography" (ECCL) is gratefully acknowledged.

References

[1] L.G. Christophorou, J.K. Olthoff, Appl. Surf. Sci. 192 (2002) 309.
[2] C. Makochekanwa, H. Kato, M. Hoshino, H. Cho, M. Kimura, O. Sueoka, H. Tanaka, Eur. Phys. J. D 35 (2005) 249.
[3] 5th EU—Japan Joint Symposium on plasma processing, 7–9 March 2007, Belgrade, Serbia, Journal of Physics: Conference Series 86 (2007).
[4] L. Sanche, Mass Spectrom. Rev. 21 (2002) 349.
[5] L. Sanche, Eur. Phys. J. D 35 (2005) 367.
[6] B. Boudaïffa, P. Cloutier, D. Hunting, M.A. Huels, L. Sanche, Radiat. Res. 157 (2002) 227.
[7] C. König, J. Kopyra, E. Illenberger, Phys. Rev. Lett. 97 (2006) 018105.
[8] P. Swiderek, Angew. Chem. Int. Ed. 45 (2006) 4056.
[9] A. Küller, W. Eck, V. Stadler, W. Geyer, A. Gölzhäuser, Appl. Phys. Lett. 82 (2003) 3776.
[10] V. Cobut, Y. Frongillo, J.P. Patau, T. Goulet, M.-J. Fraser, J.-P. Jay-Gerin, Radiat. Phys. Chem 51 (1998) 229.
[11] St.-J. Dixon-Warren, E.T. Jensen, J.C. Polanyi, Phys. Rev. Lett. 67 (1991) 2395.
[12] J.M. Seo, S.E. Harvey, Y. Chen, J.H. Weaver, Phys. Rev. B 43 (1991) 11893.
[13] G.J. Schulz, Rev. Mod. Phys. 45 (1973) 423.
[14] E. Illenberger, Electron capture processes by free and bound molecules, in: C.-Y. Ng (Ed.), Photoionization and Photodetachment, Part II, World Scientific, Advanced Series in Physical Chemistry, vol. 10B, 1063 pp. (Chap. 19).
[15] L. Sanche, Surf. Sci. 451 (2000) 82.
[16] H. Hotop, M.-W. Ruf, M. Allan, I.I. Fabrikant, Adv. At. Mol. Opt. Phys. 49 (2003) 85.
[17] H. Abdoul-Carime, S. Gohlke, E. Illenberger, Phys. Rev. Lett. 92 (2004) 168103.
[18] S. Ptasińska, S. Denifl, P. Scheier, E. Illenberger, T.D. Märk, Angew. Chem. Int. Ed. 44 (2005) 6941.
[19] V.S. Prabhudesai, A.H. Kelkar, D. Nandi, E. Krishnakumar, Phys. Rev. Lett. 95 (2005) 143202.
[20] S. Denifl, P. Sulzer, D. Huber, F. Zappa, M. Probst, T.D. Märk, P. Scheier, N. Injan, J. Limtrakul, R. Abouaf, H. Dunet, Angew. Chem. Int. Ed. 46 (2007) 5238.
[21] S. Lacombe, F. Cemic, K. Jacobi, M.N. Hedhili, Y. Le Coat, R. Azria, M. Tronc, Phys. Rev. Lett. 79 (1997) 1146.
[22] M.N. Hedhili, M. Lachgar, Y. Le Coat, R. Azria, M. Tronc, Q.B. Lu, T.E. Madey, J. Chem. Phys. 114 (2001) 1844.
[23] R. Balog, M.N. Hedhili, F. Bournel, M. Penno, M. Tronc, R. Azria, E. Illenberger, Phys. Chem. Chem. Phys. 4 (2002) 3350.
[24] R. Balog, E. Illenberger, Phys. Rev. Lett. 91 (2003) 213201.
[25] M. Lepage, M. Michaud, L. Sanche, J. Chem. Phys. 113 (2000) 3602.
[26] M. Lepage, M. Michaud, L. Sanche, J. Chem. Phys. 107 (1997) 3478.
[27] M.C. Deschamps, M. Michaud, L. Sanche, J. Chem. Phys. 121 (2004) 4284.
[28] T. Sedlacko, R. Balog, A. Lafosse, M. Stano, S. Matejcik, R. Azria, E. Illenberger, Phys. Chem. Chem. Phys. 7 (2005) 1277.
[29] M. Orzol, T. Sedlacko, R. Balog, J. Langer, G.P. Karwasz, E. Illenberger, A. Lafosse, M. Bertin, A. Domaracka, R. Azria, Int. J. Mass Spectrom. 254 (2006) 63.
[30] S.E. Bisschop, G.W. Fuchs, A.C.A. Boogert, E.F. van Dishoeck, H. Linnartz, Astron. Astrophys. 470 (2007) 749.
[31] C.J. Bennett, R.I. Kaiser, Astrophys. J. 660 (2007) 1289.
[32] K. Ushizawa, Y. Sato, T. Mitsomuri, T. Machinami, T. Ueda, T. Ando, Chem. Phys. Lett. 351 (2002) 105.
[33] T. Strother, T. Knickerbocker, J.N. Russell Jr., J.E. Butler, L.M. Smith, R.J. Hamers, Langmuir 18 (2002) 968.
[34] N.V. Richardson, Curr. Opin. Solid State Mater. Sci. 2 (1997) 517.
[35] O. Ingólfsson, F. Weik, E. Illenberger, Int. J. Mass Spectrom. Ion Process. 155 (1996) 1.
[36] R. Balog, J. Langer, S. Gohlke, M. Stano, H. Abdoul-Carime, E. Illenberger, Int. J. Mass Spectrom. 233 (2004) 267.
[37] J. Langer, M. Stano, S. Gohlke, V. Foltin, S. Matejcik, E. Illenberger, Chem. Phys. Lett. 419 (2006) 228.
[38] J. Langer, I. Martin, G. Karwasz, E. Illenberger, Int. J. Mass Spectrom. 249–250 (2006) 477.
[39] A. Hoffman, A. Laikhtmann, S. Ustaze, M. Hadj-Hamou, M.N. Hedhili, J.-P. Guillotin, Y. Le Coat, D. Teillet Billy, R. Azria, M. Tronc, Phys. Rev. B 63 (2001) 045401.
[40] J.Y. Huang, H.G. Huang, K.Y. Lin, Q.P. Liu, Y.M. Sun, G.Q. Xu, Surf. Sci. 549 (2004) 255.
[41] J.L. Davis, M.A. Barteau, Langmuir 5 (1989) 1299.
[42] B. Parker, B. Immaraporn, A.J. Gellman, Langmuir 17 (2001) 6638.
[43] Q. Gao, J.C. Hemminger, Surf. Sci. 248 (1991) 45.
[44] R.C. Millikan, K.S. Pitzer, J. Am. Chem. Soc. 80 (1958) 3515.
[45] S. Hellebust, B. O'Riordan, J. Sodeau, J. Chem. Phys. 126 (2007) 084702.
[46] A.R. Garcia, J.L. da Silva, L.M. Ilharco, Surf. Sci. 415 (1998) 183.
[47] R.L. Redington, K.C. Lin, Spectrochim. Acta A 27 (1971) 2445.
[48] C.V. Berney, J. Am. Chem. Soc 95 (1973) 708.
[49] National Institute of Standards and Technology (NIST), http://www.nist.gov.
[50] M. Bertin, F, Duvernay, P. Theule, J.B. Bossa, F. Borget, I. Martin, E. Illenberger, A. Lafosse, T. Chiavassa, R. Azria, Phys. Chem. Chem. Phys. submitted for publication.
[51] M. Falk, J. Chem. Phys. 86 (1987) 560.
[52] K.D. Bier, H.J. Jodl, J. Chem. Phys. 86 (1987) 4406.
[53] A. Pelc, W. Sailer, P. Scheier, T.D. Märk, Vacuum 78 (2005) 631.
[54] M. Allan, J. Phys. B 39 (2006) 2939.
[55] F.A. Gianturco, R.R. Lucchese, J. Langer, I. Martin, M. Stano, G. Karwasz, E. Illenberger, Eur. Phys. J. D 35 (2005) 417.
[56] A. Pelc, W. Sailer, P. Scheier, M. Probst, N.J. Mason, E. Illenberger, T.D. Märk, Chem. Phys. Lett. 361 (2002) 277.
[57] V.S. Prabhudesai, D. Nandi, A.H. Kelkar, R. Parajuli, E. Krishnakumar, Chem. Phys. Lett. 405 (2005) 172.
[58] W. Sailer, A. Pelc, M. Probst, J. Limtrakul, P. Scheier, E. Illenberger, T.D. Märk, Chem. Phys. Lett. 378 (2003) 250.
[59] D. Forney, M.E. Jacox, W.E. Thompson, J. Chem. Phys. 119 (2003) 10814.
[60] R.D. Hunt, L. Andrews, J. Chem. Phys. 82 (1985) 4442.
[61] M. Michaud, L. Sanche, Phys. Rev. A 36 (1987) 4684.
[62] M.E. Palumbo, J. Phys.: Conf. Ser. 6 (2005) 211.